Total External Reflection X-ray Absorption Spectroscopy Reveals a Zinc Coordination Shell in Phospholipid Langmuir−Blodgett Films

Francesco d'Acapito,[†] Iouri Emelianov,[‡] Annalisa Relini,[‡] Paolo Cavatorta,[§] Alessandra Gliozzi,[‡] Velia Minicozzi,[||] Silvia Morante,[||] Pier Lorenzo Solari,[†] and Ranieri Rolandi*[,‡]

GILDA, CRG and INFM, OGG, Grenoble, France, INFM and University of Genoa, Physics Department, Genoa, Italy, INFM and University of Parma, Physics Department, Parma, Italy and INFM and University of Rome "Tor Vergata", Physics Department, Rome, Italy

Received January 22, 2002. In Final Form: April 11, 2002

We have studied the local environment of zinc in phospholipid Langmuir−Blodgett films with extended X-ray absorption fine structure spectroscopy in total reflection conditions (reflEXAFS). Mono- and multilayer films made of dilauroyl-phosphatidic acid (DLPA) and monolayer films made of dimyristoyl-phosphatidylcholine (DMPC) were deposited on quartz slides from $ZnCl_2$ solutions, and their molecular order was checked by means of X-ray reflectivity measurements. A very good signal-to-noise ratio in the reflEXAFS spectra of both multi- and monomolecular films was obtained. The theoretical fits to the experimental data show that zinc coordinates four atoms about 0.20 nm distant in both acidic DLPA and neutral DMPC films, while in water solutions, zinc coordinates six atoms about 0.21 nm distant.

Introduction

Cobalt, copper, iron, manganese, and zinc, first-row transition metals, are present in small amounts in biological systems, but they are essential to life, serving as aids to biochemical reaction catalysis and stabilizers of many biological structures.[1] Zinc is the second most abundant metal after iron. It has many different functions and may interact with biological molecules in different ways forming with its ligands different coordination polyhedra. Zinc binds negatively charged residues (e.g., carboxylates and thiolates) via charge−charge interactions and neutral residues (e.g., carbonyls and imidazoles) via orientation-dependent charge−dipole interactions, with coordination numbers varying between 4 and 6. In aqueous solutions, zinc binds six water molecules and exists as a hexahydrate, $Zn^{2+}(OH_2)_6$, while in proteins it mostly resides in tetrahedral or distorted tetrahedral sites. Cysteine and histidine are the most preferred ligands. Histidine is mainly found when zinc plays a catalytic role. In these cases, zinc is exposed to bulk solvent and typically binds one of the solvent molecules and its coordination number may increase to 5 during an enzymatic turnover.[2]

Biomimetic chemistry also takes advantage of zinc coordination capabilities, for instance, in the preparation of biomimetic membranes according to the Langmuir−Blodgett (LB) method. This method permits the sequential deposition of ordered mono- and multimolecular layers on solid substrates starting from a monomolecular film of an insoluble surfactant spread at the air−water interface. LB films of long-chain fatty acids and acidic phospholipids are more easily prepared in the presence of divalent cations in the subphase. Since zinc is particularly effective in promoting film deposition, it is widely used in LB preparation. In Zn−arachidate films, the zinc layers have been precisely localized between the lipid polar heads by using the X-ray standing wave method.[3−5] The "in-plane" and "out-of-plane" molecular order of these films was determined by atomic force microscopy[6] and X-ray diffraction[7] measurements, respectively.

Extended X-ray absorption fine structure spectroscopy (EXAFS) is a technique widely used on solid-state samples to investigate the local structure around selected atomic species.[8] Due to the remarkable penetrating power of hard X-rays, this technique naturally probes the bulk of the investigated material. Surfaces and interfaces can, instead, be probed by setting the sample in total external reflection conditions (reflEXAFS) so that the radiation might be confined in a layer a few nanometers thick. The intensities of both the reflected beam and fluorescence signal allow measurement of the absorption coefficient of the material inside the probed thin layer.[9,10] Despite the fact that in this configuration EXAFS can be very effective to study the local atomic environment of metal ions in organic films, it is rarely used to this aim.[11,12]

* To whom correspondence should be addressed. Department of Physics, University of Genoa, Via Dodecaneso 33, 16146 Genoa, Italy. Phone: +39-010-3536424. Fax: +39-010-314218. E-mail: rolandi@fisica.unige.it.

[†] GILDA, CRG and INFM, OGG.

[‡] INFM and University of Genoa.

[§] INFM and University of Parma.

[||] INFM and University of Rome "Tor Vergata".

(1) Mathews, C. K.; van Holde, K. E. *Biochemistry*; Benjamin/Cummings Publishing: Redwood City, CA, 1990; pp 7−10.

(2) Christianson, D. W. *Adv. Protein Chem.* **1991**, *42*, 281.

(3) Bedzyk, M. J.; Bilderback, D. H.; Bommarito, G. M.; Caffrey, M.; Schildkraut, J. S. *Science* **1988**, *241*, 1788.

(4) Wang, J.; Bedzyk, M. J.; Penner, T. L.; Caffrey, M. *Nature* **1991**, *354*, 377.

(5) Itri, R.; Zhang, R.; Caffrey, M. *Biophys. J.* **1997**, *73*, 1506.

(6) Viswanathan, R.; Madsen, L. L.; Zasadzinski, J. A.; Schwartz, D. K. *Science* **1995**, *269*, 51.

(7) Dhanabalan, A.; Prasanth-Kumar, N.; Major, S.; Talwar, S. S. *Thin Solid Films* **1998**, *327−329*, 787.

(8) Lee, P. A.; Citrin, P. H.; Eisenberger, P.; Kincaid, B. M. *Rev. Mod. Phys.* **1981**, *53*, 769.

(9) Parratt, L. G. *Phys. Rev.* **1954**, *95*, 359.

(10) Heald, S. M.; Chen, H.; Tranquada, J. M. *Phys. Rev.* **1988**, *B38*, 1016.

(11) Oyanagi, H.; Yoneyama, M.; Ikegami, K.; Sugi, M.; Kuroda, S.-I.; Ishiguro, T.; Matsushita, T. *Thin Solid Films* **1988**, *159*, 435.

(12) Tageuchi, S.; Nagami, Y.; Ishiguru, T.; Oyanagi, H. *Thin Solid Films* **1994**, *250*, 243.

10.1021/la025564q CCC: $22.00
Published on Web 05/15/2002

We used reflEXAFS to study zinc coordination in Langmuir−Blodgett films of 1,2-dilauroyl-*sn*-glycero-3-phosphate (DLPA) and 1,2-dimyristoyl-*sn*-glycero-3-phosphocholine (DMPC). We chose these lipids since we wanted to compare the behavior of charged and uncharged phospholipids. At the air−water interface and at pH values ranging from 5 to 7, DLPA monolayers are negatively charged, while DMPC monolayers are zwitterionic. To test the sensitivity of the technique, we have performed measurements on monomolecular films (DLPA and DMPC) and we have compared the data with those obtained from a 21-layer film (DLPA). The film structures were checked by X-ray reflectivity measurements.

EXAFS

The EXAFS signal function is the relative variation of the X-ray absorption coefficient of the material, μ, with respect to the absorption coefficient of the inspected atomic species, μ_0:

$$\chi(k) = \frac{\mu(k) - \mu_0(k)}{\mu_0(k)} \tag{1}$$

Both are functions of the modulus of the photoelectron wave vector, k,

$$k = \sqrt{\frac{2m_e(E - E_0)}{\hbar^2}} \tag{2}$$

where m_e is the electron mass and E_0 is the ionization energy. In the present study (see Materials and Methods), the EXAFS signal has been measured from the fluorescence intensity that is proportional to the absorption coefficient in the case of diluted samples.

The theoretical EXAFS signal is calculated as a function of the parameters that describe the photoelectron backscattering process by the neighboring atoms. In the single scattering approximation, the formula reads

$$\chi(k) = \sum_j \frac{N_j}{kR_j^2} A_j(k) \sin[2kR_j + \Phi_j(k)] e^{-2k^2\sigma_j^2} e^{-\lambda k} \tag{3}$$

where the sum is over the j atomic coordination shells. N_j is the number of neighbors in the jth shell, R_j is their mean distance from the absorber and σ_j is the corresponding Debye−Waller factor, λ is the mean free path of the photoelectron, k is the modulus of the photoelectron wave vector, and $A_j(k)$ and $\Phi_j(k)$ are the backscattering amplitude and phases, respectively. In this paper, N_j, R_j, and σ_j have been obtained by the best fit of the experimental data, while $A_j(k)$ and $\Phi(k)$, which can be extracted from the analysis of the spectra of some structurally known compound, have been ab initio computed. The term containing the mean free path, λ, was included in the backscattering amplitude.

Materials and Methods

Sample Preparation. DLPA and DMPC (purity > 99%) were purchased from Avanti Polar Lipids (Alabaster, AL) and used without further purification. Langmuir monolayers were formed in a Nima trough (Coventry, U.K.) by spreading the lipids, dissolved in organic solvents, on 2 mM $ZnCl_2$ unbuffered solutions, whose pHs resulted to be about 5.5. The organic solvents (Aristar-grade BDH, Milan, Italy) were chloroform−methanol 3:1 (v/v) for DLPA and chloroform for DMPC. Milli-Q (Millipore, Bedford, MA) filtered water with resistivity larger than 18 MΩ cm was used.

Monolayers were transferred onto hydrophilic quartz slides (10 × 40 mm^2, Hellma Italia, Milan, Italy) by vertical dipping. The surface pressure was kept constant at 30 and 10 mN/m for DLPA and DMPC, respectively. We chose to deposit DMPC monolayers at a lower pressure since we observed a slight area instability when these monolayers were kept at higher pressure. The deposition procedure started with the quartz slide immersed in the subphase. The layers exposing hydrophobic tails were deposited during upstrokes (odd layers), while the layers exposing hydrophilic groups were deposited during downstrokes (even layers). Only one layer of DMPC could be deposited. The deposition rate of the first layer was 1 mm/min. For successive layers, the rate was gradually increased up to 16 mm/min. After every odd layer deposition, the sample was allowed to dry in air for a few minutes. The deposition ratio was approximately 1 for each stroke. The bare quartz slide densities and roughness measured by X-ray reflectivity are 2.20 g/cm^3 and 0.39 nm, respectively, in excellent agreement with the data provided by Hellma.

X-ray Reflectivity Measurements. X-ray reflectivity measurements have been performed with a butterfly-type X-ray reflectometer assembled at the Department of Physics of Genoa University. The mechanical parts, provided by JJ X-Ray, Denmark, are actuated by stepping motors remote controlled by the TASCOM software package through an ECB electronic interface (Risø National Laboratory, Roskilde, Denmark, and JJ X-Ray). The reflectometer, primarily developed to perform measurements on films at gas−liquid interfaces, was adapted to solid substrates. In this configuration, the incident angle can be varied from 0° to 7° with minimum steps of 0.0003°.

The reflectometer is equipped with a conventional X-ray glass tube (PW 2273/20, Long Fine Focus, Cu anode, PW 1316 tube shield, Philips Analytical) fed by a PW 1830/40 high-power generator (Philips Analytical). Typically, the tube is operated at 40 kV and 55 mA to obtain the maximum intensity. A Ni filter cuts the Cu Kβ line and lets the Cu Kα line (0.15417 nm) pass through an attenuator made up of Cu foils to suitably reduce the beam intensity. Both the incident and reflected beam are confined in Newport evacuated flight tubes sealed with Kapton windows. The incident beam is collimated by two pairs of vertical and horizontal slits mounted on the flight tube extremes. The reflected beam intensity is detected by an energy-dispersive Si detector (Amptek Inc., Bedford, MA). A pair of slits, before the detector, cut off the diffuse scattering background.

The detector is connected to a multichannel analyzer (MULTIPORT-16E/R, Oxford Instruments Inc., Nuclear Measurements Group, Oak Ridge, TN), whose output is connected to the ECB counter. The reflectometer setup allows reflectivity measurements down to $R \sim 10^{-7}$. The experimental data were analyzed with IMD software developed by David L. Windt, provided by ESRF (Grenoble, France) as a part of the XOP 2.0 (X-ray Oriented Programs) software package.[13]

EXAFS Measurements. EXAFS measurements at the Zn K-edge (9659 eV) were performed at the GILDA CRG beamline of the European Synchrotron Radiation Facility (Grenoble, France). The monochromator was equipped with a Si(311) crystal pair with the second sagittally bent and run in dynamic focusing mode. The harmonic rejection was achieved by slightly changing the angle of the first crystal with respect to the second (crystal detuning) to reduce the beam intensity to 70% of the maximum by working at 70% of the reflectivity curve. The beam was sized to 40 μm by a pair of slits placed 2 m apart to limit the residual divergence. The incoming beam was monitored from the fluorescence of a thin Ti foil. The reflectivity was measured by a Si PIN diode, whereas the fluorescence from the sample was measured with a 1 cm^2 single-element High Purity Ge detector placed at 4 cm from the sample. Prior to EXAFS measurements, reflectivity scans below the edge were done in order to determine the optimum angle that maximizes the fluorescence yield. In all cases, this value was about 0.2°, corresponding to a footprint on the sample of 11 mm. Due to the dilution of the absorbing species in the sample, no effects due to self-absorption or δ-EXAFS[10] were observable.

(13) Windt, D. L. *Comput. Phys.* **1998**, *12*, 360.

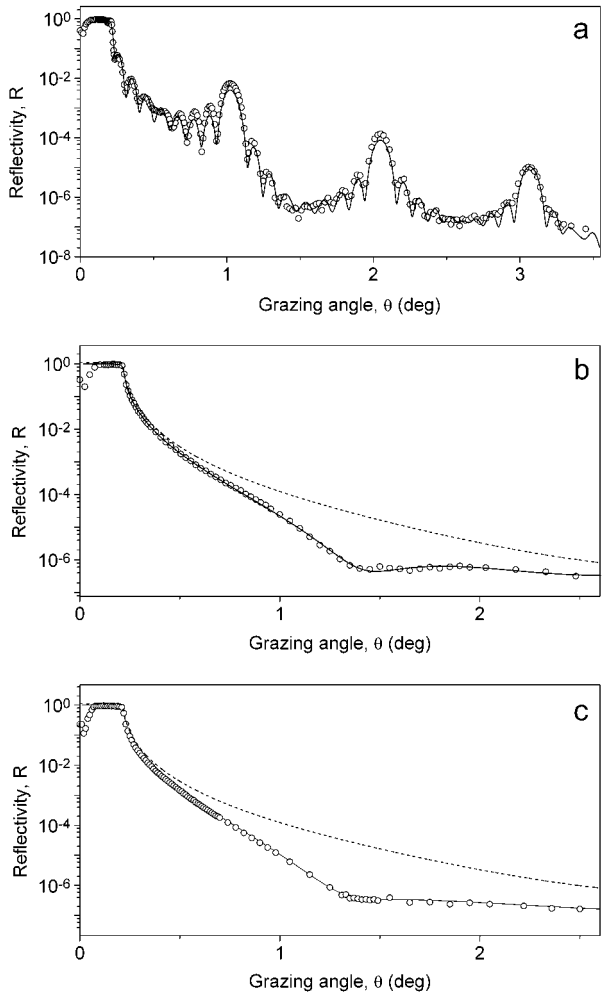

Figure 1. X-ray reflectivity curves of LB films deposited on quartz slides from 2 mM $ZnCl_2$ unbuffered solutions (pH ~ 5.5): (a) DLPA, 19 layers; (b) DLPA, 1 layer; (c) DMPC, 1 layer. Circles, experimental data; continuous lines, best fits; dashed lines, substrate best fits.

Results and Discussion

Reflectivity Measurements. A few reflectivity scans were performed at GILDA before reflEXAFS measurements in order to determine the critical angle. The GILDA apparatus was not optimized for reflectivity measurements, and its angle resolution did not allow determination of the film structure with sufficient accuracy. To obtain accurate information on the film structure, we performed reflectivity measurements with the reflectometer assembled in Genoa on samples prepared with the same materials and the same procedures. These high-resolution data, which we report in the following, are in good agreement with the low-resolution data recorded at GILDA. This fact, together with the well-established reproducibility of the deposition procedure, legitimates the assumption that the samples used in the two different experiments have indeed the same structure.

Figure 1 shows the reflectivity curves of three different LB films: panel a, a 19-layer DLPA film; panel b, a 1-layer DLPA film; and panel c, a 1-layer DMPC film. In panel a, the most pronounced maximums are the main Bragg peaks caused by the interference of the signals reflected by the electronically denser parts of the film, which are the hydrophilic moieties with bound zinc. The spacing, d, between these adjacent layers is provided by the equation

$$d = \lambda/2(\sin\theta_{n+1} - \sin\theta_n) \quad (4)$$

where λ is the X-ray wavelength and θ_{n+1} and θ_n are the angular positions of two adjacent Bragg peaks. At angles immediately larger than the critical angle and around the main Bragg peaks, Kiessig oscillations become visible. They are caused by the interference of the signals reflected by the substrate−film interface and by the film−air interface. Their angular distance provides the film's total thickness according to eq 4. Since surface roughness rapidly damps the Kiessig oscillations, they are visible only if the film surface is relatively smooth.

We used the density box model[14] to fit the experimental data. Each lipid monomolecular layer was considered as made of two sublayers of different density corresponding to the polar region and the alkyl chain, respectively. The sublayer edges were smoothed by taking into account interface roughness. Each sublayer was characterized by three parameters: density, thickness, and roughness. To reduce the number of free parameters, all inner layers were regarded as identical. In the fitting procedure, we estimated the initial guess values of these parameters in the following way. The polar region density was calculated considering a few different models with different Zn−DLPA ratios (from 0.5:1 to 1:1) and different hydration shells. The length of the hydrocarbon chain in the all-trans configuration was estimated to be 1.38 nm from the equation

$$l\,(\mathrm{nm}) = (n \times 0.125 + 0.1265) \quad (5)$$

where n is the number of CH_2 groups, 0.125 nm is the contribution to the chain length of each CH_2 group, and 0.1265 nm is the contribution of the terminal CH_3 group.[15] In the all-trans configuration, the full length of DLPA, which has $n = 10$, results to be 2.20 nm, having assigned the value of 0.8235 nm to the polar head length as reported by Lukes, Petty, and Yarwood.[16]

The bilayer spacing ($d = 4.33$) nm was calculated from angular distances between Bragg peaks, the total film thickness (D = 420 nm) was calculated from angular distances between Kiessig fringes, and the average film density ($\rho = 1.22$ g/cm^3) was calculated from the critical angle position.

To select among the models with different polar region densities, the first fit runs were performed keeping constant the parameters obtainable directly from the experimental data such as the bilayer spacing, the total film thickness, and the average film density. Eventually, we allowed all parameters to change freely. Through χ^2 minimization, the best fit was obtained for the 1:1:4.9 Zn/DLPA/H_2O complex. The other fit parameters are reported in Table 1. The hydrophobic region thickness that comes from the fit is smaller than the theoretical estimate of about 0.08 nm. This discrepancy, which is outside of the measure confidence interval, can be explained with alkyl chain tilting, imperfect all-trans configuration, and partial interdigitation of the alkyl chains. From the nominal mass of the hydrophobic tail and its density and thickness, obtained by the fit procedure, the area per molecule of DLPA results to be 0.433 ± 0.010 nm^2, which is in good agreement with that

(14) Als-Nielsen, J.; Möhwald, H. In *Handbook of Synchrotron Radiation*; Ebashi, S., Koch, M., Rubestein, E., Eds.; Elsevier Science: Amsterdam, 1991; Vol. 4, pp 1−53.
(15) Lohner, K.; Konovalov, O. V.; Samoilenko, I. I.; Myagkov, I. V.; Troitzky, V. I.; Berzina, T. I. *Thin Solid Films* **1996**, *288*, 262.
(16) Lukes, P. J.; Petty, M. C.; Yarwood, J. *Langmuir* **1992**, *8*, 3043.

Table 1. Structure Parameters of the 19-Layer DLPA Film[a]

Monolayer Average Parameters			
sublayers	density (g/cm^3)	thickness (nm)	monolayer total thickness (nm)
apolar layer	0.915 ± 0.015	1.303 ± 0.008	2.163 ± 0.018
polar layer	1.685 ± 0.025	0.860 ± 0.01	

Film Parameters						
			roughness (nm)			
density (g/cm^3)	bilayer spacing (nm)	thickness (nm)	σ_{in} [b]	σ_{up} [b]	area per molecule (nm^2/mol)	number of H_2O molecules per lipid molecule
1.22 ± 0.02	4.33 ± 0.04	41.1 ± 0.3	0.14 ± 0.02	0.67 ± 0.03	0.433 ± 0.010	4.9 ± 1.0

[a] The uncertainties correspond to the 68% confidence interval of the χ^2 value (ref 26). [b] σ_{in} and σ_{up} are the roughness of the inner interfaces and upper layer, respectively.

Table 2. Structure Parameters of the 1-Layer DLPA and DMPC Films[a]

lipid	sublayers	density (g/cm^3)	thickness (nm)	monolayer total thickness (nm)	area per molecule (nm^2/mol)	number of H_2O molecules per lipid molecule
DLPA	apolar layer	0.89 ± 0.02	1.36 ± 0.04	2.51 ± 0.13	0.427 ± 0.022	16 ± 5
	polar layer	1.94 ± 0.05	1.14 ± 0.09			
DMPC	apolar layer	0.73 ± 0.04	1.34 ± 0.04	2.30 ± 0.11	0.626 ± 0.053	8.6 ± 5.5
	polar layer	1.45 ± 0.05	0.97 ± 0.07			

[a] The uncertainties correspond to the 68% confidence interval of the χ^2 value (ref 26).

measured from monolayer isotherms at the air−water interface (0.43 ± 0.02 nm^2).

Even in the case of the DLPA monolayer, the best-fit results are consistent with a 1:1 (Zn/DLPA) complex, but in this case the uncertainty is large. From polar region density and area per lipid molecule, the polar group molecular mass results to be 568 Da. Subtracting the mass for the 1:1 complex (290.4 Da), we have a residual mass of 277.6 Da that should be associated with captured water and Zn ions. The exact chemical composition of this hydrate complex is unknown. Disregarding Zn ions, it corresponds to about 16 molecules of water per lipid molecule. In this case, a relatively thick layer of water should be adsorbed on the substrate surface. In agreement with this finding, we observed a polar region thickness larger than the expected one. Instead, the thickness of the hydrophobic region is very close to the theoretical estimate, suggesting that hydrocarbon chains are oriented perpendicularly to the substrate. The values of the fit parameters are consistent with an area per molecule of 0.427 ± 0.022 nm^2 that is in good agreement with the area per molecule measured from isotherms at the deposition pressure.

The fit of DMPC monolayer reflectivity data was performed by assuming a 1:1:5 (Zn/DMPC/H_2O) complex, as suggested for 1-palmitoyl-2-oleoyl-phosphatidylcholine (POPC) that has the same polar group.[17] The hydrophobic region thickness was 1.6265 nm from eq 5, and the polar region thickness was 1.0235 nm from the dipalmitoyl-phosphatidylcholine (DPPC) data given by Lohner et al.[15]

The results of the best fit are reported in Table 2. They are consistent with a 1:1:9 (Zn/DMPC/H_2O) complex. The area per molecule of 0.626 ± 0.053 nm^2 is, within the experimental errors, equal to that provided by the isotherms at the air−water interface at the deposition pressure (0.64 ± 0.03 nm^2).

The hydration shell of 8.6 ± 5.5 water molecules per DMPC molecule is in good agreement with the value (8.9) obtained by Hollinshead et al.[18] from neutron reflectivity measurements on a LB monolayer deposited on silicon oxide. The thickness of DMPC hydrocarbon chains provided by the fit is somewhat smaller than the theoretical value for the all-trans configuration and corresponds to a tilt of 34.8° with respect to the normal to the film plane. This relatively large tilt angle is justified by the relatively low deposition pressure.

The polar region thickness of 0.97 ± 0.07 nm is in good agreement with the values obtained by other authors who found the phosphatidylcholine headgroup length to be 0.80 ± 0.15 nm in bilayers of both DPPC and distearoyl-phosphatidylcholine (DSPC) on a silicon substrate[19,20] and bilayers of DMPC on a quartz substrate[20] and 0.94 nm in a monolayer of DMPC on a hydrophobized silicon substrate.[17] The total film thickness of 2.30 ± 0.11 nm is in agreement with the thickness of 4.60 ± 0.15 nm of a DMPC bilayer in the L-beta phase (t = 20 °C) on a quartz substrate.[21]

ReflEXAFS Measurements. The raw reflEXAFS spectra are shown in Figure 2, whereas the relative Fourier transforms (FT) are reported in Figure 3. Curves a and b correspond to the samples of 21 and 1 molecular layers of DLPA, respectively, while curve c corresponds to the DMPC monolayer. A ratio of roughly 20 was observed between the fluorescence yields of the multilayer and monolayer samples: this is due to the fact that by maximizing the fluorescence, the X-ray beam penetrated the whole layer in both cases.

The FT spectra are consistent with a single Zn coordination shell. Quantitative data analysis has been done with an ab initio approach using the UWXAFS package.[22] First, the backscattering potential was calculated on the base of a local cluster around the central Zn atoms derived from the ZnO structure.[23] The theoretical EXAFS signals were then calculated and compared with the EXAFS spectrum of a 4 mM $ZnCl_2$ aqueous solution, obtaining in this way a good agreement (see Table 3) with previously reported results.[24] Spectra relative to the samples were

(17) Binder, H.; Arnold, K.; Ulrich, A. S.; Zschörning, O. *Biophys. Chem.* **2001**, *90*, 57.
(18) Hollinshead, C. M.; Hanna, M.; Barlow, D. J.; De Biasi, V.; Bucknall, D. G.; Camilleri, P.; Hutt, A. J.; Lawrence, M. J.; Lu, J. R.; Su, T. J. *Biochim. Biophys. Acta* **2001**, *1511*, 49.
(19) Charitat, T.; Bellet-Amalric, E.; Fragneto, G.; Graner, F. *Eur. Phys. J. B* **1999**, *8*, 583.
(20) Reinl, H.; Brumm, T.; Bayerl, T. M. *Biophys. J.* **1992**, *61*, 1025.
(21) Johnson, S. J.; Bayerl, T. M.; McDermott, D. C.; Adam, G. W.; Rennie, A. R.; Thomas, R. K.; Sackmann, E. *Biophys. J.* **1991**, *59*, 289.
(22) Zabinsky, S. I.; Rehr, J. J.; Ankudinov, A.; Albers, R. C.; Eller, M. J. *Phys. Rev.* **1995**, *B52*, 2995.
(23) Wychoff, R. N. G. *Crystal Structures*; Wiley: New York, 1964.
(24) Kuzmin, A.; Obst, S.; Purans, J. *J. Phys.: Condens. Matter* **1997**, *9*, 10065.

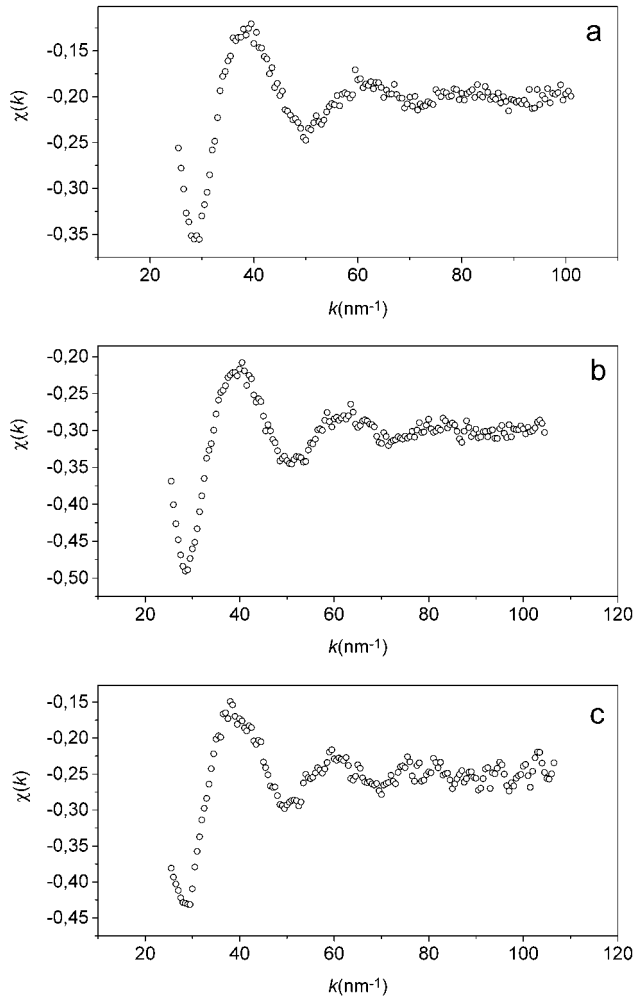

Figure 2. ReflEXAFS spectra of DLPA and DMPC LB films: (a) DLPA, 21 layers; (b) DLPA, 1 layer; (c) DMPC, 1 layer.

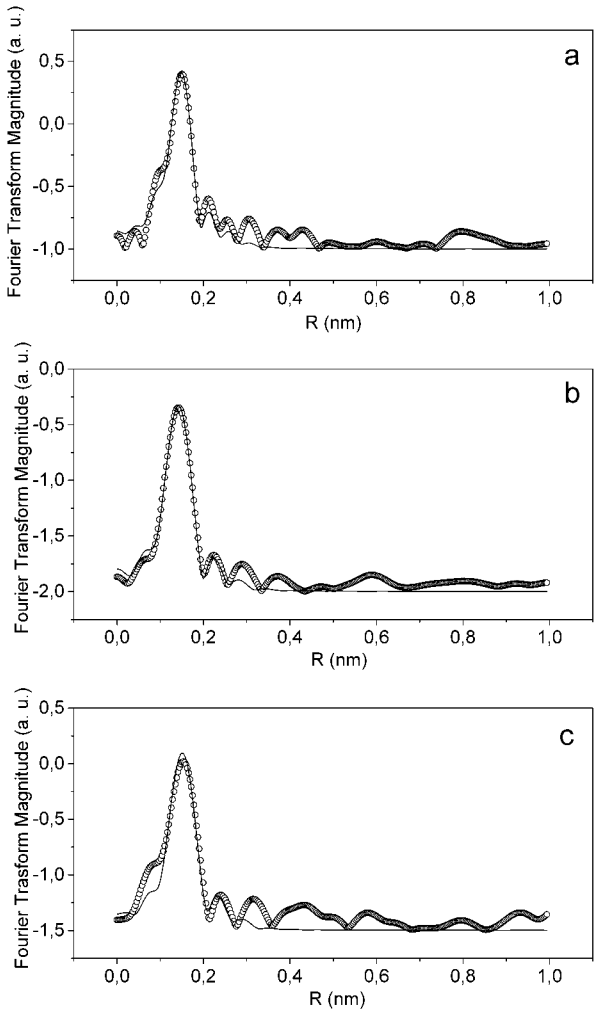

Figure 3. Fourier transforms of the reflEXAFS spectra shown in Figure 2: (a) DLPA, 21 layers; (b) DLPA, 1 layer; (c) DMPC, 1 layer. Continuous lines are best fits.

extracted with standard procedures, Fourier transformed in the k range between 24 and 80 nm^{-1} and fitted directly in R space between 0.06 and 0.20 nm with a single Zn−O shell. The comparison of these spectra with those of Zn^{2+} ions in aqueous solution shows that all of the former exhibit both a lower Zn−O coordination number and a shorter bond length. The latter compares well with the Zn−O separation $R = 0.154$ nm observed in a glassy system containing tetrahedral Zn.[25] Our data clearly show that a hexahedral Zn site such as that in aqueous solutions has to be ruled out. The expected Zn−O−P structure is not detectable with our data, probably because of a marked configurational disorder caused by the spread of the values of the Zn−O−P bond angles.

There are two main results of these measurements that we want to point out. The first one is that there is no difference between the Zn^{2+} coordination numbers in charged and uncharged phospholipids, and the second one is that the coordination number in the membrane, 4, is different from that in aqueous solution, 6. Both of these results confirm the observation of Binder and co-workers, based on IR linear dichroism and gravimetric measurements,[17] that Zn^{2+} interacts strongly with the lipid headgroup by binding directly the phosphate group independently of the anionic or zwitterionic nature of the lipid. This fact should not be regarded as a contradiction to the common finding that anionic lipids enhance the Zn^{2+} effects in biological and artificial membranes. The effects of zinc ions also depend on their concentration at the solution membrane interface which is increased by the strong attractive Coulomb forces between anions and acidic lipids.

Table 3. Zinc Coordination Shell Parameters[a]

sample[b]	N[c]	R (nm)[c]	σ^2 (10^{-5} nm^2)[d]
DLPA (21)	3.4 ± 0.7	0.199 ± 0.003	3 ± 5
DLPA (1)	3.8 ± 0.7	0.195 ± 0.003	0 ± 5
DMPC (1)	3.8 ± 0.7	0.202 ± 0.003	1 ± 5
aqueous solution	6.5 ± 0.7	0.211 ± 0.003	8 ± 2

[a] The uncertainties correspond to the 68% confidence interval of the χ^2 value (ref 26). [b] The numbers in parentheses are the layer numbers. [c] N is the number of neighbors in the first coordination shell, and R is their distance from the zinc ion. [d] σ is the Debye−Waller factor.

The second result, also, agrees with Binder and co-workers'[17] observation that Zn ions and lipid molecules lose part of their hydration shell when they bind each other. Binder and co-workers showed that zinc forms either 2:1 or 1:1 complexes with phospholipid molecules binding the negatively charged phosphate groups. As a consequence of Zn^{2+} binding, the C−O−P−O−C− backbone of the lipid headgroup changes from gauche/gauche into trans/trans conformation and it loses roughly 50% of the

(25) Matz, W.; Stachel, D.; Goremychkin, E. A. *J. Non-Cryst. Solids* **1988**, *101*, 80.
(26) Lampton, M.; Margon, B.; Bowyer, S. *Astrophys. J.* **1976**, *208*, 177.

hydration shell. At a relative humidity of ~71%, 1 mol of pure ZnCl and 1 mol of pure phospholipid take up ~7 mol of water each. The mixture of the two components binds about 5 water molecules per lipid. The decrease of the Zn coordination number after binding is indicative that the Zn ion loses its shell of water molecules to coordinate itself with the phosphate oxygen atoms.

At the present stage of our investigation, we cannot distinguish which oxygen atoms form the Zn coordination shell, if one or more water molecules take part of the shell, and which is the local order around the Zn ion. It is likely that the Zn ion coordinates with lipid molecules belonging to both the same (cis) and the opposite layer (trans), concurring with the in-plane and trans-plane order of the film. Water molecules should also be very important to stabilize the overall structure.

The fact that the Zn coordination number is similar for monolayers and multilayers could suggest that the cis layer determines the Zn coordination. The presence of oxygen atoms on the substrate surface and of water molecules between the substrate and the lipid layer makes the substrate−lipid interface similar to the polar lipid−lipid interface so that the Zn ion local atomic environment is very similar in both of the interfaces. If phosphorus atoms concur to form the second coordination shell, this should be different for monolayers and multilayers since the glass substrates do not contain phosphorus.

Interestingly, the Zn coordination number turns out to be equal in monolayers and multilayers even if the amount of water bound to the first monolayer and entrapped between the lipid polar region and the quartz substrate seems to be much higher than that bound to the inner layers. However, to conclude that the Zn coordination number is independent of the amount of bound water, further investigation is required.

Conclusions

X-ray reflectivity and reflEXAFS measurements indicate that zinc ions form 1:1 complexes with phospholipid molecules in LB films and that the first coordination shell is formed by 3−4 oxygen atoms. The mean distance of these atoms from the zinc ion is about 0.2 nm. This scenario is similar for acidic (DLPA) and zwitterionic (DMPC) lipids both deposited from unbuffered subphases at pH 5.5.

Acknowledgment. The reflEXAFS experimental results have been obtained during the LS-1728 experiment at the GILDA CRG beamline of the European Synchrotron Radiation Facility (Grenoble, France).

LA025564Q